

Microsecond spin-flip times in *n*-GaAs measured by time-resolved polarization of photoluminescence

J. S. Colton,* T. A. Kennedy, A. S. Bracker, and D. Gammon
Naval Research Laboratory, Washington, DC 20375, USA

(Received 24 September 2003; published 23 March 2004)

We have observed microsecond spin-flip times in lightly doped *n*-GaAs, by measuring the photoluminescence polarization in the time domain with pump and probe pulses. Times up to 1.4 μ s have been measured. Our results as a function of magnetic field indicate three regions governing the spin relaxation: a low field region, where spin-flip times increase due to suppression of the nuclear hyperfine interaction for localized electrons, a medium field region where spin-flip times increase due to narrowing of the hyperfine relaxation for interacting electrons, and a high field region where spin-flip times begin to level off due to the increasing importance of spin-orbit relaxation mechanisms.

DOI: 10.1103/PhysRevB.69.121307

PACS number(s): 72.25.Rb, 72.25.Fe, 78.55.Cr, 71.55.Eq

The study of spin in semiconductors has become important in recent years for potential applications such as spintronics and quantum computing.¹ GaAs is being considered as a material for quantum computing, and recent observations of electron spin dephasing times in the hundreds of nanosecond range in *n*-type GaAs have been encouraging.^{2–4} This is particularly true since the spin properties of electrons localized on donors bear similarities to those of electrons localized in quantum dots, the latter being key components of possible scalable solid-state quantum computing schemes.⁵ The focus in this paper is on spin properties of doped electrons in lightly doped *n*-GaAs.

There have been theoretical predictions for spin lifetimes in *n*-GaAs. Theoretical values for the inhomogeneous spin dephasing time T_2^* range from a few to a few hundred nanoseconds,⁴ but the homogeneous dephasing time T_2 may be in the microseconds regime.^{6–8} Similarly, the spin-flip time τ_S , has been predicted to be microseconds or even longer.^{9,10} Note that these predictions do not hold for fully delocalized conduction electrons—spin dephasing and spin-flip times in that case are predicted to be only in the tens of nanoseconds.¹¹

Experimentally, the T_2^* values in *n*-GaAs have been measured through a variety of ways: the decay envelope of the time resolved Faraday rotation signal,² the width of Hanle effect curves,^{3,4,12,13} and the width of magnetic resonance curves.¹⁴ These values agree well with theory. The T_2 time has not yet been measured, and the only measurements of which we are aware of for τ_S in such systems have yielded a value of 50 μ s or longer at 20 mK and 7.5 T by transport measurements in lithographically defined gated quantum dots.¹⁵

In this work, we have used the well-known connection between spin polarization and optical polarization¹⁶ to measure spin-flip times in two *n*-GaAs samples via time resolved polarization of photoluminescence (PL). This type of spectroscopy has also been used to measure spin-flip times ranging from \sim 100 ps to 20 ns in *p*-GaAs and *p*-GaAs-related materials,^{17–19} \sim 1 ns in InGaAs quantum disks,²⁰ and most recently 15 ns in *n*-InAs/GaAs self assembled quantum dots.²¹ We have extended the technique into the microsecond

regime. The spin-flip times are longest at low temperature and high fields, and times up to 1.4 μ s were observed.

We believe that this is an important measurement for several reasons. First, the times we have observed are long compared to other times measured in GaAs. Second, these long times are obtained at moderate fields and only moderately low temperatures. Third, electrons under these conditions are fairly well localized. Finally, these experiments imply a possibility for employing microwave pulses in conjunction with the light pulses to perform a spin echo T_2 measurement in the future.

The samples we investigated were one micron thick GaAs layers in an AlGaAs heterostructure, whose growth and characteristics are described elsewhere.¹³ Two different doping levels were studied: 1 and 3×10^{15} cm⁻³. All of the data presented here is for the 3×10^{15} cm⁻³ sample, although the results for the 1×10^{15} cm⁻³ sample are both quantitatively and qualitatively similar.

We used circularly polarized light from a Ti-sapphire laser at 809 nm to inject spin polarized electrons. The sample was placed in a superconducting magnet and cooled to liquid helium temperatures. Photoluminescence was collected with a double grating spectrometer and measured with a two-channel photon counter (PC). Due to the rapid spin exchange between electrons,²² the optical polarization of the free exciton PL reflects the spin polarization of donor electrons.²³

The laser was operated in cw mode, but its intensity was modulated on/off with a fast acousto-optic modulator (AOM) to obtain light pulses as short as 15 ns. The AOM was controlled by the voltage pulses of a digital word generator (WG), which in turn was controlled by a computer program to change the spacing and/or duration of the pulses. The WG was triggered by a 20 kHz photoelastic modulator (PEM) in the PL detection path. The PEM operated as an oscillating quarter-wave plate, which combined with a linear polarizer to make a circular polarization analyzer. The PEM additionally triggered the two channels of the counter so that the two polarizations σ^+ and σ^- could be separately recorded. The PL polarization was then established by dividing the difference of the two channels by their sum: $P = (\sigma^+ - \sigma^-) / (\sigma^+ + \sigma^-)$.

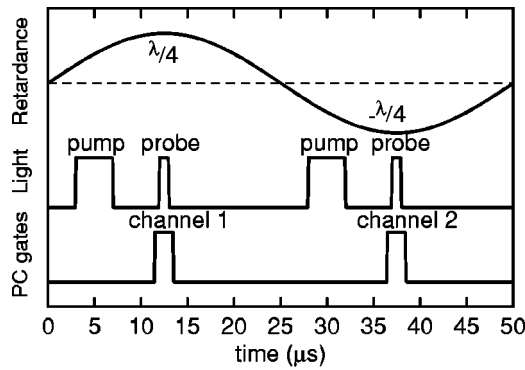


FIG. 1. The timing sequences showing the light pulses and photon counter gates, relative to the PEM retardance. Gate 1 and gate 2 count the σ^+ and σ^- of the probe pulse PL, respectively.

In the experiment, four light pulses were employed: a pump pulse, a probe pulse detecting σ^+ , then after a long delay a second pump pulse followed by a second probe pulse detecting σ^- . The pulses were arranged so that the probe pulse (and PC gates) were centered on the max/min of PEM retardance (see Fig. 1). Note that the difference between pump and probe pulses is obtained through varying the pulse width, rather than the pulse intensity²⁴ as is more common in two-beam pump-probe spectroscopy.^{2,21} Also, since the electron spins are only partially ($\sim 5\%$) aligned for at most $\sim 10\%$ of the repetition period, the average electronic polarization is close to the thermal equilibrium value; thus effects from the dynamic polarization of the nuclei (the Overhauser effect) are not important for these experiments.

Simple rate equations can be used to describe the spin-flips of a two level system.²⁵ For a transition rate of w_{12} (w_{21}) for transitions from state 1 to state 2 (2 to 1), the rate equations for the populations N_1 and N_2 at any time are

$$\frac{dN_1}{dt} = N_2 w_{21} - N_1 w_{12}, \quad \frac{dN_2}{dt} = N_1 w_{12} - N_2 w_{21} = -\frac{dN_1}{dt}. \quad (1)$$

Relaxation processes bring the system into thermal equilibrium. In this condition,

$$\frac{N_1^{\text{eq}}}{N_2^{\text{eq}}} = \frac{w_{21}}{w_{12}} = e^{-E_{12}/kT}, \quad (2)$$

where E_{12} is the energy difference between the two levels. In our experiments, the pump pulse produces nonequilibrium populations N_1^0 and N_2^0 at time zero. Using the above equations, it can be shown that the population difference ($N_1 - N_2$) will evolve toward thermal equilibrium following a simple exponential law:

$$[N_2(t) - N_1(t)] - [N_2^{\text{eq}} - N_1^{\text{eq}}] = [(N_2^0 - N_1^0) - (N_2^{\text{eq}} - N_1^{\text{eq}})] e^{-t/\tau_s}, \quad (3)$$

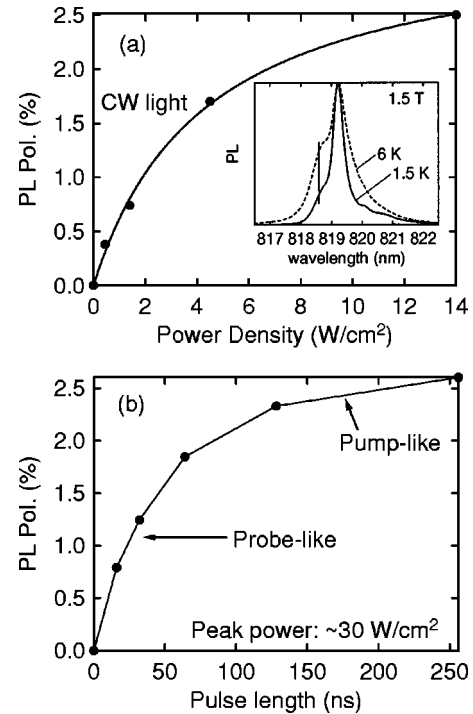


FIG. 2. PL polarization for (a) cw and (b) pulsed laser excitation. (a) The degree of polarization vs the laser power density at $B=0$ T and $T=6$ K. The fit (solid line) is described in Ref. 13. The inset shows normalized PL spectra at 1.5 T for temperatures of 1.5 and 6 K. The vertical bar marks the position of the free exciton. (b) The degree of polarization vs the length of a single pulse, for $B=0$ T and $T=6$ K.

where $\tau_s = (w_{12} + w_{21})^{-1}$. The experiments gave exponential decays for the change in population difference in all cases, and thus are well described by this characteristic spin-flip time, τ_s .

The cw PL of sample 3E15 at 1.5 T is displayed in the inset to Fig. 2(a) for two different temperatures. The free exciton line (lower wavelength) is polarized to a degree that depends strongly on the cw laser power density, as shown in Fig. 2(a). This follows the well-known dependence for n -type samples.¹⁶ A similar effect is seen if the power density is held constant while the pulse length changes: see Fig. 2(b). The number of injected photoelectrons must be comparable to the number of doped electrons in order for an appreciable polarization to be set by the light pulse. This allows us to set conditions for pump and probe pulses: the pump pulse must replace many electrons already present in the material (obtained for pulse lengths $>$ about 200 ns in the figure); the probe pulse must replace very few ($<$ about 50 ns). Note that the probe pulse does not measure the system without affecting it—it is also circularly polarized, and results in a PL polarization of about 1%. Thus for less-doped samples, weaker probe beams are required, but are correspondingly more difficult to detect.

Our pump-probe spectroscopy was performed using 16 ns probe pulses and 256 ns pump pulses. As the pump-probe delay was increased, the polarization decayed exponentially from the pump to the probe value, in accordance with Eq. (3).²⁶ Some representative decays are shown in Fig. 3, per-

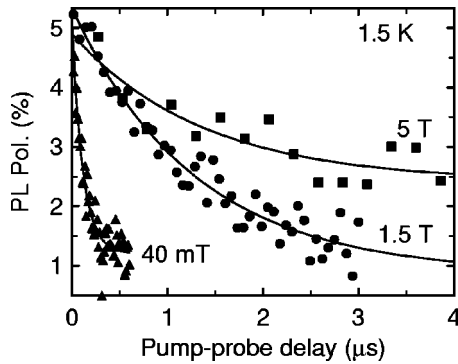


FIG. 3. Change in detected PL polarization vs pump-probe delay for $T=1.5$ K and fields of 0.04, 1.5, and 5 T. Solid lines are exponential fits to the data with decay times of 0.11, 1.28, and 1.37 μs , respectively.

formed at 1.5 K at magnetic field values of 0.04, 1.5, and 5 T. The corresponding τ_S values are 0.11, 1.3, and 1.4 μs , respectively.

A summary of the measured τ_S values at various fields and temperatures is presented in Figs. 4(a) and 4(b). The times decrease with temperature and increase with magnetic field. There are three distinguishable magnetic field ranges: (1) low field, less than ~ 0.1 T, (2) medium field, between 0.1 and ~ 1.5 T, and (3) high field, greater than 1.5 T. Figure 4(a) is a log-log plot showing all three ranges. Figure 4(b) is a

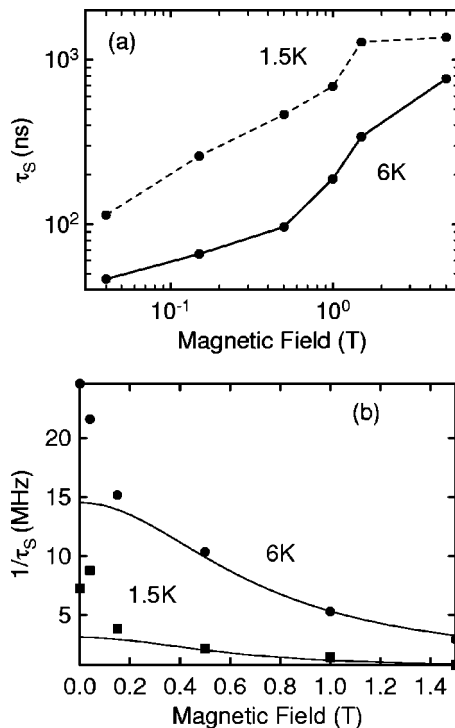


FIG. 4. Summary of the spin-flip measurements showing (a) the spin-flip times including the highest fields on a log scale, and (b) the spin-flip rates at the smallest fields (including $B=0$) on a linear scale. In (b), the middle field range for each temperature is fit to a Lorentzian shape as discussed in the text. The Lorentzian widths are 0.60 and 0.70 T for the 1.5 K and 6 K data, respectively.

linear plot of $1/\tau_S$ vs B to emphasize the first two ranges. The middle field region of each curve in Fig. 4(b) has been fit to a Lorentzian centered at 0 T; the widths obtained by the fit were 0.60 and 0.70 T for the 1.5 and 6 K data, respectively.

Before commenting on our data, we point out that there is a natural distribution of donor separations, which can lead to more- and less-localized electrons. Application of a magnetic field, however, tends to localize electrons due to cyclotron motion. Thus at low fields, a distinction between types of electrons—localized versus interacting—may be made, but at high fields this distinction will disappear. We believe the three regimes mentioned above correspond to (1) localized electrons at low fields, (2) interacting electrons at slightly higher fields, and (3) localized electrons at high fields.

The observed τ_S lifetimes at zero field should be equal to T_2^* , since there is no energy splitting between the two spin states. Our τ_S values do indeed fit well with the T_2^* times observed previously by our group and others.^{2,4,13,14} For localized electrons, the main relaxation mechanism under these conditions is hyperfine coupling to the nuclei. Specifically, the hyperfine interaction produces an effective magnetic field (the “fluctuation field”) in which an electron precesses.⁶ In the quantum dot case, and in the low doping limit of *n*-GaAs, the inhomogeneity in this effective field limits the observed spin coherence times to roughly 5 ns. However, as an external magnetic field is applied, the nuclear contribution to relaxation will be reduced when the external field exceeds the nuclear fluctuation field. This is a possible explanation for our data in the $B < 0.1$ T range, and would imply that our samples do in fact contain some very highly localized electrons.

For concentrations such that electrons at different donor sites can interact, the average hyperfine field an electron sees is reduced and the spin-flip time can become much longer. The averaging is characterized by a “correlation time,” τ_c , which is a measure of the interaction between donors due to electron hopping or electron spin exchange. The inverse, $1/\tau_c$, is a measure of the rate of change in the local magnetic field which an *individual* electron sees.²⁷ In the motional-averaging regime, τ_S will increase with B , with $1/\tau_S$ following a Lorentzian dependence: $\tau_S^{-1} \propto (B^2 + B_c^2)^{-1}$, where B_c depends explicitly on the correlation time: $B_c = \hbar/g\mu_B\tau_c$. The widths of the Lorentzian fits from Fig. 4(b) (0.60 and 0.70 T) correspond to correlation times of $\tau_c = 43$ and 37 ps for $T = 1.5$ and 6 K, respectively. These values are very close to those deduced by Dzhioev *et al.* for this doping regime.⁴ Thus the field dependence in the middle range of fields arises from motional averaging of the hyperfine effects for interacting electrons.

As magnetic field is increased further, this simple model does not work. The correlation time, for example, is not constant, and must increase as the electrons become localized due to the field. Moreover, the Larmor frequency increases with field and becomes comparable to $1/\tau_c$ at fields of a few tesla, so a model in which τ_S is set due to interactions with the local nuclear field must break down. In the previous model, however, we have neglected the spin-orbit terms of the Hamiltonian. These obviously cannot be completely neglected in GaAs—the *g* value is far from 2, which indicates there is an admixture of the orbital angular momentum into

the spin up and spin down states. This admixture, plus the spin-orbit interaction leads to spin-lattice relaxation if phonons are present.

Calculations of spin-orbit interaction have been made for GaAs quantum dots. In Khaetskii and Nazarov's calculation, the dominant contribution to spin-flips is shown to be due to this admixture of spin states and spin-orbit interaction, with a B^5 dependence of spin flip rate on magnetic field.⁹ Woods *et al.* have similarly done calculation for quantum dots, and give $1/\tau_S$ relaxation rates via one-phonon (B^5 dependencies) and two-phonon mechanisms (no strong B dependence, dominant at higher temperatures).¹⁰ Although these results may not be directly applicable to donors in bulk GaAs, it seems likely that the relaxation rates in that case will similarly be field-independent or increasing with field. With the hyperfine-related relaxation rates decreasing with field, at some point these phonon-related rates will become dominant. We believe that the leveling off of the 1.5 K data at high field is an indication that we have indeed reached that point.

In conclusion, we have measured spin relaxation times in n -GaAs for various field and temperature values, and the longest times exceed $1 \mu\text{s}$. The field dependence of the spin-flip times displays three regions governed by different mechanisms. The long spin-flip times are an exciting and important result, particularly since they are for modest fields and temperatures. The technique we used may find applicability with other samples. It should also be possible to combine this type of pulsed light experiment with a pulsed microwave resonance experiment—the microwaves occurring between pump and probe pulses—in order to perform a spin echo measurement of T_2 . However, it is clear that the field range for such a resonance experiment will have to be higher than in our previous optically polarized and detected spin resonance.¹⁴

The authors thank A.I.L. Efros, T.L. Reinecke, and L.M. Woods for helpful discussions. J.S.C. was supported by NRC and NRL. Work has also been supported by DARPA and ONR.

*Current address: Physics Department, U.W. La Crosse, La Crosse WI 54601.

¹S. A. Wolf, D. D. Awschalom, R. A. Buhrman, J. M. Daughton, S. von Molnar, M. L. Roukes, A. Y. Chtchelkanova, and D. M. Treger, *Science* **294**, 1488 (2001).

²J. M. Kikkawa and D. D. Awschalom, *Phys. Rev. Lett.* **80**, 4313 (1998).

³R. I. Dzhioev, V. L. Korenev, I. A. Merkulov, B. P. Zakharchenya, D. Gammon, A. L. Efros, and D. S. Katzer, *Phys. Rev. Lett.* **88**, 256801 (2002).

⁴R. I. Dzhioev, K. V. Kavokin, V. L. Korenev, M. V. Lazarev, B. Ya. Meltser, M. N. Stepanova, B. P. Zakharchenya, D. Gammon, and D. S. Katzer, *Phys. Rev. B* **66**, 245204 (2002).

⁵D. Loss and D. P. DiVincenzo, *Phys. Rev. A* **57**, 120 (1998).

⁶I. A. Merkulov, A. L. Efros, and M. Rosen, *Phys. Rev. B* **65**, 205309 (2002).

⁷R. de Sousa and S. Das Sarma, *Phys. Rev. B* **67**, 033301 (2003).

⁸A. Khaetskii, D. Loss, and L. Glazman, *Phys. Rev. B* **67**, 195329 (2003).

⁹A. V. Khaetskii and Y. V. Nazarov, *Phys. Rev. B* **64**, 125316 (2001).

¹⁰L. M. Woods, T. L. Reinecke, and Y. Lyanda-Geller, *Phys. Rev. B* **66**, 161318 (2002).

¹¹F. X. Bronold, I. Martin, A. Saxena, and D. L. Smith, *Phys. Rev. B* **66**, 233206 (2002).

¹²R. I. Dzhioev, B. P. Zakharchenya, V. L. Korenev, and M. N. Stepanova, *Phys. Solid State* **39**, 1765 (1997).

¹³J. S. Colton, T. A. Kennedy, A. S. Bracker, and D. Gammon, *Phys. Status Solidi B* **233**, 445 (2002).

¹⁴J. S. Colton, T. A. Kennedy, A. S. Bracker, D. Gammon, and J. B. Miller, *Phys. Rev. B* **67**, 165315 (2003).

¹⁵T. Fujisawa, Y. Tokura, and Y. Hirayama, *Phys. Rev. B* **63**,

081304 (2001); R. Hanson, B. Witkamp, L. M. K. Vandersypen, L. H. Willems van Beveren, J. M. Elzerman, and L. P. Kouwenhoven, *Phys. Rev. Lett.* **91**, 196802 (2003).

¹⁶See, e.g., *Optical Orientation*, edited by F. Meier and B. P. Zakharchenya (North-Holland, Amsterdam, 1984).

¹⁷For the rate equations for photoelectrons, see R. J. Seymour and R. R. Alfano, *Appl. Phys. Lett.* **37**, 231 (1980).

¹⁸J. Wagner, H. Schneider, D. Richards, A. Fischer, and K. Ploog, *Phys. Rev. B* **47**, 4786 (1993).

¹⁹T. Endo, K. Sueoka, and K. Mukasa, *Jpn. J. Appl. Phys., Part 1* **39**, 397 (2000).

²⁰H. Gotoh, H. Ando, H. Kamada, A. Chavez-Pirson, and J. Temmyo, *Appl. Phys. Lett.* **72**, 1341 (1998).

²¹S. Cortez, O. Krebs, S. Laurent, M. Senes, X. Marie, P. Voisin, R. Ferreira, G. Bastard, J.-M. Gérard, and T. Amand, *Phys. Rev. Lett.* **89**, 207401 (2002).

²²D. Paget, *Phys. Rev. B* **24**, 3776 (1981); **25**, 4444 (1982).

²³V. B. Vekua, R. I. Dzhioev, B. P. Zakharchenya, and V. G. Fleisher, *Sov. Phys. Semicond.* **10**, 210 (1976).

²⁴In practice, probe beams shorter than ~ 20 ns caused the AOM to switch the light off before it had completely finished switching it on, and were thus reduced in peak intensity by $\sim 1/3$ compared to longer pulses.

²⁵B. di Bartolo, *Optical Interactions in Solids* (Wiley, New York, 1968), p. 345.

²⁶At small fields this would be entirely due to dynamic polarization of the electrons; at large fields there was a large thermal polarization on which the dynamic portion was superimposed. In general, we measured the PL polarization for both σ^+ and σ^- excitation, then subtracted the two to remove the thermal background and obtain the dynamic portion of the polarization which is discussed in the text and shown in Fig. 3.

²⁷M. I. D'yakonov and V. I. Perel', *Sov. Phys. JETP* **38**, 177 (1974).